THE JOURNAL OF PHYSICAL CHEMISTRY A LETTERS

**2008,** *112,* 790−793
Published on Web 01/11/2008

# Resonance Hyper-Raman Scattering of Fullerene $C_{60}$ Microcrystals

**Katsuyoshi Ikeda* and Kohei Uosaki**

*Division of Chemistry, Graduate School of Science, Hokkaido University, Sapporo 060-0810, Japan*

*Received: October 19, 2007; In Final Form: December 26, 2007*

The hyper-Raman spectrum of buckminsterfullerene $C_{60}$ was observed at room temperature. The spectrum clearly showed infrared-active modes with $t_{1u}$ symmetry and the silent modes with $t_{2u}$, $g_u$, and $h_u$ as a result of electronic resonances via the Herzberg−Teller mechanism. Moreover, Raman-active modes with $a_g$ and $h_g$ were also detected, although these were hyper-Raman-forbidden in the electric dipole approximation, suggesting a contribution of higher-order nonlinear processes such as magnetic dipole transitions. These results suggest that hyper-Raman spectroscopy and microscopy are indeed widely applicable in the field of molecular science.

## 1. Introduction

Buckminsterfullerene $C_{60}$, the "most beautiful molecule",[1] has attracted much attention since its discovery in 1985 because of its unique properties such as third-order optical nonlinearity, superconductivity, and ferromagnetism.[2−6] These properties are related to the highly delocalized and strongly correlated $\pi$-electrons in the spherical cage with the icosahedral $I_h$ symmetry. It is of great importance to study such a high degenerate electron-vibration coupling in the field of material science from the viewpoint of fundamental aspects and applications. In spite of many theoretical and experimental efforts,[7] our understanding of fullerenes is still limited because of the elaborate network of the coupled electronic and vibrational structures. Resonance vibrational spectroscopy is one of the most powerful tools to probe such an electron-vibration coupled system. According to the group theory, $C_{60}$ has 174 internal degrees of freedom with 46 distinct vibrational coordinates having the representation.[8]

$$\Gamma_{vib} = 2a_g + 1a_u + 3t_{1g} + 4t_{1u} + 4t_{2g} + 5t_{2u} + 6g_g + 6g_u + 8h_g + 7h_u \quad (1)$$

The numbers of infrared- and Raman-active modes are 4 ($4t_{1u}$) and 10 ($2a_g + 8h_g$), respectively. All other modes are infrared- and Raman-forbidden modes ($a_u$, $t_{1g}$, $t_{2g}$, $t_{2u}$, $g_g$, $g_u$, $h_u$) and are called silent modes. Although conventional vibrational spectroscopy such as "one-photon" IR absorption and "two-photon" Raman scattering cannot access such silent modes, higher-order optical processes, e.g., three- and four-photon Raman scattering, can probe those directly because of less restrictive selection rules in nonlinear optical processes.[9] Moreover, multiphoton Raman scattering can utilize electronic resonances in order to enhance the scattering intensity. Combination of resonance two-photon Raman (ordinary Raman) scattering and resonance three-photon Raman (hyper-Raman) scattering is expected to be useful to collect full information of the electron-vibration coupled system.

Hyper-Raman scattering, which is an inelastic second-order nonlinear process, is due to hyperpolarizability modulations by nuclear vibrations of molecules:

$$\beta_{ijk} = \beta^0_{ijk} + \sum_l (\partial\beta_{ijk}/\partial Q_l)_0 Q_l + ... \quad (2)$$

where the hyperpolarizability $\beta$ is represented as the expansion in the series of the normal coordinates $Q$ near the equilibrium $\beta^0$ and the second term is responsible for hyper-Raman.[10] The selection rules of hyper-Raman are rather similar to IR; all infrared-active modes and some of the silent modes are hyper-Raman-active. For the $C_{60}$ molecule of $I_h$ symmetry, the number of active modes is 22 ($4t_{1u} + 5t_{2u} + 6g_u + 7h_u$), and these are mutually exclusive with Raman-active modes. In spite of the characteristic feature of the selection rules, spectroscopic application has been very limited because of the extremely small scattering cross section.[11] For many researchers, therefore, microscopic application of hyper-Raman scattering has been out of consideration except for a few examples.[12−14]

This Letter reports microscopic observation of resonance hyper-Raman scattering from microcrystalline $C_{60}$ at room temperature, indicating the potentiality of hyper-Raman spectroscopy and microscopy. The observed hyper-Raman peaks were in good agreement with theoretical predictions, showing the direct spectroscopic observation of the silent modes. Moreover, Raman-active modes were also found in the spectrum, suggesting a higher-order contribution.

## 2. Experimental Section

A mode-locked Ti:sapphire laser (Spectra-Physics, Tsunami) with a custom-made laser line filter (Optical Coatings Japan) was used to excite crystalline $C_{60}$ for observation of hyper-Raman scattering. A pulse radiation of 0.05 nJ with a pulse width of 14 $cm^{-1}$ full width at half-maximum (fwhm) (a pulse duration of ~1 ps) was introduced into an inverted microscope system (Nikon, TE-2000) with a 100×, 1.49 N.A. oil-immersion microscope objective. Back scattered photons were collected by the same objective and filtered by dichroic mirrors (Optical Coatings Japan). Note that surface second-harmonic generation

* Corresponding author. E-mail: kikeda@pchem.sci.hokudai.ac.jp.

10.1021/jp710147g CCC: $40.75 

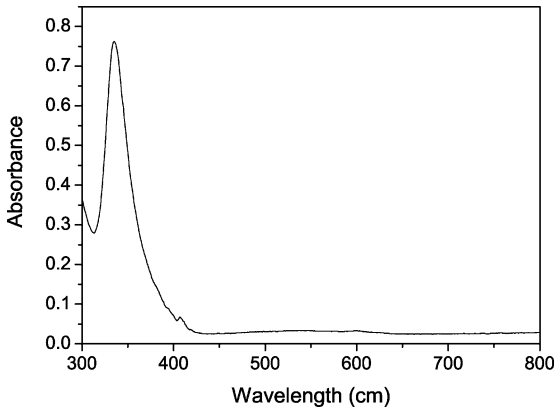


**Figure 1.** UV−vis absorption spectrum of $C_{60}$ molecules in toluene.

from the coverslip was negligible because the incident angle was normal to the surface. Finally, hyper-Raman signals were detected by a charge-coupled camera (Princeton Instruments, PIXIS:400B) with a polychromator (ACTON, SP2500i). The exposure time for recording the hyper-Raman spectrum was 30 min.

Microcrystalline films of $C_{60}$ molecules (Strem Chemicals, Inc., 99.9% grade) were obtained on a coverslip by evaporation of $C_{60}$-saturated toluene solution. Figure 1 shows a UV−vis spectrum of $C_{60}$−toluene solution, exhibiting a very intense dipole-allowed $^1T_{1u}-^1A_g$ transition band around 340 nm and a very weak dipole-forbidden lowest transition band around 550 nm.[15,16]

### 3. Results and Discussion

$C_{60}$ molecules are known to occupy face-centered cubic (fcc) lattice points in the solid phase, resulting in symmetry lowering from $I_h$ to $T_h$.[17] However, the symmetry lowering perturbation is almost negligible at room temperature. This is because intermolecular van der Waals forces are much weaker than the intramolecular covalent forces within individual molecules and, therefore, molecules at room temperature are freely rotating in the lattice.[18]

Figure 2 shows vibrational modes of $C_{60}$ microcrystals probed by the conventional vibrational spectroscopy, Raman scattering and IR absorption. The Raman spectrum, which was measured by excitation with a 785 nm CW radiation of a diode laser, showed all of the Raman-active modes, $2a_g + 8h_g$. Conversely, the IR spectrum, taken by the KBr pellet method, clearly showed the IR-active modes, $4t_{1u}$. Since both spectra were consistent with the theoretical calculations of a free $C_{60}$ molecule,[19] one can assume that the symmetry lowering in the solid is negligible in the following hyper-Raman spectroscopy.

Figure 3 shows the hyper-Raman spectrum of the crystalline $C_{60}$ (we confirmed that there was no contribution from the coverslip to the spectrum). Peak positions of theoretically calculated hyper-Raman-active and Raman-active modes are also marked with black and gray bars in the spectrum. The most intense peak at 0 $cm^{-1}$ is due to hyper-Rayleigh scattering, which probably originates from magnetic dipole contributions, i.e., the magnetic dipole-allowed two-photon upward and electric dipole-allowed one-photon downward transitions between $^1T_{1u}$ and $^1A_g$.[20] In the Stokes shift region, several peaks appeared: intense stretching vibrational modes around 1300−1600 $cm^{-1}$ and bending vibrations around 500−800 $cm^{-1}$. Compared with the theoretical calculation, all of the hyper-Raman-active modes of the icosahedral $C_{60}$, i.e., the infrared-active $t_{1u}$ and the silent $t_{2u}$, $g_u$, and $h_u$, were seen in the spectrum. Moreover, Raman-

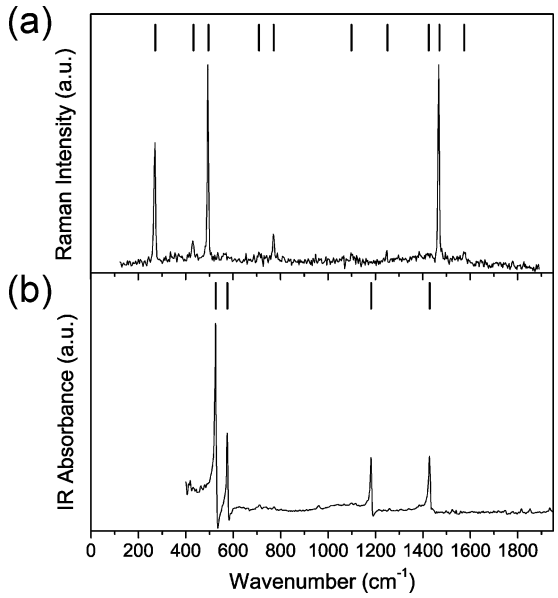


**Figure 2.** (a) Raman spectrum of $C_{60}$ microcrystals excited by 785 nm diode laser radiation. (b) IR absorption spectrum of $C_{60}$ microscystals, taken by the KBr method. Theoretically calculated Raman-active and IR-active modes are marked in the spectra.[19]

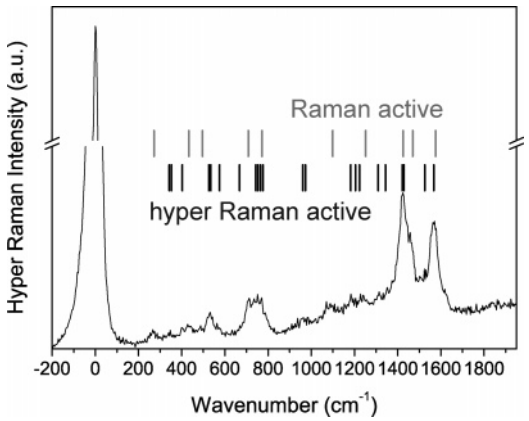


**Figure 3.** Hyper-Raman spectrum of $C_{60}$ microcrystals excited by 790 nm pulse radiation from the Ti:sapphire laser, with theoretically calculated hyper-Raman-active modes (black bars) and Raman-active modes (gray bars).[19]

active modes, which should be inactive in hyper-Raman scattering under the electric dipole approximation, were also found to appear in the spectrum; for example, the 270 $cm^{-1}$ peak was obviously associated with the lowest mode of $C_{60}$, the Raman-active $h_g(1)$ mode. The possibility of photodegradation or photopolymerization of $C_{60}$ molecules[21] was excluded by Raman observation after the hyper-Raman measurement. Table 1 summarizes the recommended values[19] for the 46 distinct normal-mode frequencies of $C_{60}$ molecule and the obtained values by using Raman, IR, and hyper-Raman scattering in this work.

The magnitude of hyper-Raman scattering cross sections is typically of the order of $10^{-65}$ $cm^4$•s, and thus, it is quite difficult to obtain a spectrum under an off-resonant condition in a microscopic measurement system. It can be assumed that the obtained spectrum was enhanced by electronic resonances (see Figure 1). In the case of centrosymmetric molecules such as $C_{60}$, the Herzberg−Teller contribution is the leading term for resonance hyper-Raman processes while the Frank−Condon-type transition is forbidden in the electric dipole approximation.[22] Considering the incident energy ($\hbar\omega$ = 1.57 eV) and

**TABLE 1: Recommended Values for the 46 Distinct Normal-Mode Frequencies of the $C_{60}$ Molecule in ref 19 and the Obtained Values by Using Raman Scattering (RS), IR Absorption (IR), and Hyper-Raman Scattering (HRS) in This Work**

| symmetry | frequency ($cm^{-1}$)[19] | RS ($cm^{-1}$) | IR ($cm^{-1}$) | HRS ($cm^{-1}$) |
|---|---|---|---|---|
| hg(1) | 272 | 271 | | 270 |
| t2u(1) | 342 | | | 340 |
| gu(1) | 353 | | | 348 |
| hu(1) | 403 | | | 400 |
| hg(2) | 433 | 432 | | 432 |
| gg(1) | 485 | | | |
| ag(1) | 496 | 495 | | 492 |
| t1u(1) | 526 | | 526 | 531 |
| hu(2) | 534 | | | |
| t2g(1) | 553 | | | |
| gg(2) | 567 | | | |
| t1g(1) | 568 | | | |
| t1u(2) | 575 | | 575 | 573 |
| hu(3) | 668 | | | |
| hg(3) | 709 | 709 | | 710 |
| gg(3) | 736 | | | |
| hu(4) | 743 | | | 736 |
| t2u(2) | 753 | | | 751 |
| t2g(2) | 756 | | | |
| gu(2) | 764 | | | |
| hg(4) | 772 | 770 | | 771 |
| gu(3) | 776 | | | 776 |
| t2g(3) | 796 | | | |
| t1g(2) | 831 | | | |
| gu(4) | 961 | | | 968 |
| t2u(3) | 973 | | | |
| Au | 984 | | | |
| gg(4) | 1079 | | | |
| hg(5) | 1099 | 1097 | | 1096 |
| t1u(3) | 1182 | | 1181 | 1182 |
| t2u(4) | 1205 | | | |
| hu(5) | 1223 | | | 1225 |
| hg(6) | 1252 | 1250 | | |
| t1g(3) | 1289 | | | |
| gu(5) | 1309 | | | 1310 |
| gg(5) | 1310 | | | |
| hu(6) | 1344 | | | 1351 |
| t2g(4) | 1345 | | | |
| gu(6) | 1422 | | | 1421 |
| hg(7) | 1425 | 1426 | | |
| t1u(4) | 1429 | | 1428 | |
| ag(2) | 1470 | 1468 | | 1466 |
| gg(6) | 1482 | | | |
| t2u(5) | 1525 | | | 1524 |
| hu(7) | 1567 | | | 1564 |
| hg(8) | 1575 | 1574 | | 1574 |

the electronic states of $C_{60}$, there are two possibilities for the Herzberg−Teller-type intensity borrowing. One possible resonance is two-photon allowed upward and vibronic one-photon allowed downward transitions between the excited state $^1H_g$ and the ground state $^1A_g$; the two-photon energy level of the incidence is on the edge of the two-photon absorption band.[23] Another possible resonance is vibronic two-photon allowed upward and one-photon allowed downward transitions between the excited state $^1T_{1u}$ and the ground state $^1A_g$. At present, it is difficult to determine which state dominantly contributed to the enhancement without information on the wavelength dependence. In contrast with the obvious enhancement mechanism of the hyper-Raman-active modes, the appearance of Raman-active modes is not simply explained as long as the electric dipole approximation is considered; these Raman-active modes are forbidden in hyper-Raman scattering processes even if the symmetry lowering perturbation to the fcc $T_h$ is taken into account. Therefore, a higher-order contribution has to be additionally considered. As already mentioned, the magnetic dipole transition is known to contribute to the *elastic* hyper-Rayleigh scattering of $C_{60}$ molecules. Therefore, it can be assumed that magnetic dipole-allowed two-photon upward and electric dipole-allowed one-photon downward transitions between $^1T_{1u}$ and $^1A_g$ contributed to the *inelastic* hyper-Raman scattering, in which Raman-active modes are allowed.

The silent modes of $C_{60}$ have been observed by inelastic neutron scattering, high-resolution electron energy loss, and low-temperature fluorescence spectroscopy in neon and argon matrixes.[19] Compared with these techniques, however, hyper-Raman is more widely applicable in various experimental conditions because it does not require ultrahigh vacuum or low-temperature conditions. Isotopic perturbations are also sometimes utilized for spectroscopic activation of silent modes, but electron-vibration coupling properties may be simultaneously broken. Direct optical observation under the different selection rules should be useful in molecular science.

## 4. Conclusion

We have observed the vibrational modes of the solid $C_{60}$ at room temperature by using the hyper-Raman scattering technique. The spectrum showed very rich vibrational structures including both the hyper-Raman-active and Raman-active modes. The scattering intensity of the hyper-Raman-active modes was resonantly enhanced by Herzberg−Teller contribution in the electric dipole transitions. Conversely, the appearance of the Raman-active modes was probably due to the Frank−Condon-type mechanism of the magnetic dipole two-photon upward and electric dipole one-photon downward transitions.

Potential application of hyper-Raman spectroscopy is very attractive. In principle, it can be an alternative of IR absorption spectroscopy, which is applicable even in IR opaque media and can benefit by electronic resonances. For example, we have already obtained a preliminary result of hyper-Raman study of single-walled carbon nanotubes, suggesting a possible use as chirality-selective spectroscopy for IR-active mode detection.[14] Hyper-Raman spectroscopy is now becoming a practically useful spectroscopic tool for molecular science.

**Acknowledgment.** This research was partially supported by a Grant-in-Aid for Scientific Research (A) (2006-2009, No. 18205016) and by the Global COE Program (Project No. B01: Catalysis as the Basis for Innovation in Materials Science) from the Ministry of Education, Culture, Sports, Science and Technology, Japan.

## References and Notes

(1) Aldersey-Williams, H. *The Most Beautiful Molecule: The Discovery of the Buckyball*; John Wiley & Sons: New York, 1995.

(2) Kroto, H. W.; Heath, J. R.; O'Brien, S. C.; Curl, R. F.; Smalley, R. E. *Nature* **1985**, *318*, 162.

(3) Meth, J. S.; Vanherzeele, H.; Wang, Y.; *Chem. Phys. Lett.* **1992**, *197*, 26.

(4) Hebard, A. F.; Rosseinsky, M. J.; Haddon, R. C.; Murphy, D. W.; Glarum, S. H.; Palstra, T. T. M.; Ramirez, A. P.; Kortan, A. R. *Nature* **1991**, *350*, 600.

(5) Allemand, P.-M.; Khemani, K. C.; Koch, A.; Wudl, F.; Holczer, K.; Donovan, S.; Grüner, G.; Thompson, J. D. *Science* **1991**, *253*, 301.

(6) Rao, A. M.; Zhou, P.; Wang, K.-A.; Hager, G. T.; Holden, J. M.; Wang, Y.; Lee, W.-T.; Bi, X.-X.; Eklund, P. C.; Cornett, D. S.; Duncan, M. A.; Amster, I. J. *Science* **1993**, *259*, 955.

(7) Dresselhaus, M. S.; Dresselhaus, G.; Eklund, P. C. *Science of Fullerenes and Carbon Nanotubes*; Academic Press: San Diego, CA, 1996.

(8) Weeks, D. E.; Harter, W. G. *J. Chem. Phys.* **1989**, *90*, 4744.

(9) Christie, J. H.; Lockwood, D. J. *J. Chem. Phys.* **1971**, *54*, 1141.

(10) Denisov, V. N.; Mavrin, B. N.; Podobedov, V. B. *Phys. Rep.* **1987**, *151*, 1.

(11) Kneipp, J.; Kneip, H.; Kneipp, K. *Proc. Natl. Acad. Sci. U.S.A.* **2006**, *103*, 17149.
(12) Shimada, R.; Kano, H.; Hamaguchi, H. *Opt. Lett.* **2006**, *31*, 320.
(13) Ikeda, K.; Takase, M.; Sawai, Y.; Nabika, H.; Murakoshi, K.; Uosaki, K. *J. Chem. Phys.* **2007**, *127*, 111103.
(14) Ikeda, K.; Saito, Y.; Hayazawa, N.; Kawata, S.; Uosaki, K. *Chem. Phys. Lett.* **2007**, *438*, 109.
(15) Hare, J. P.; Kroto, H. W.; Taylor, R. *Chem. Phys. Lett.* **1991**, *177*, 394.
(16) László, I.; Udvardi, L. *Chem. Phys. Lett.* **1987**, *136*, 418.
(17) Heiney, P. A.; Fischer, J. E.; McGhie, A. R.; Romanow, W. J.; Denenstein, A. M.; McCauley, J. P., Jr.; Smith, A. B., III; Cox, D. E. *Phys. Rev. Lett.* **1991**, *66*, 2911.
(18) Yannoni, C. S.; Johnson, R. D.; Meijer, G.; Bethune, D. S.; Salem, J. R. *J. Phys. Chem.* **1991**, *95*, 9.
(19) Menéndez, J.; Page, J. B. In *Light Scattering in Solids VIII*; Cardona M., Güntherodt, G., Eds.; Springer: Berlin, 2000.
(20) Koopmans, B.; Janner, A.-M.; Jonkman, H. T.; Sawatzky, G. A.; van der Woude, F. *Phys. Rev. Lett.* **1993**, *71*, 3569.
(21) Rao, A. M.; Zhou, P.; Wang, K.-A.; Hager, G. T.; Holden, J. M.; Wang, Y.; Lee, W.-T.; Bi, X.-X.; Eklund, P. C.; Cornett, D. S.; Duncan, M. A.; Amster, I. J. *Science* **1993**, *259*, 955.
(22) Chung, Y. C.; Ziegler, L. D. *J. Chem. Phys.* **1988**, *88*, 7287.
(23) Banfi, G. P.; Fortusini, D.; Bellini, M.; Milani, P. *Phys. Rev. B* **1997**, *56*, R10075.